AXIAL WAVE PROPAGATION IN TRUNCATED CONES

by

BHUMIL A. DIWANJI

Presented to the Faculty of the Graduate School of

The University of Texas at Arlington in Partial Fulfillment

of the Requirements

for the Degree of

MASTER OF SCIENCE IN MECHANICAL ENGINEERING

THE UNIVERSITY OF TEXAS AT ARLINGTON

DECEMBER 2010

ACKNOWLEDGEMENTS

Firstly and importantly I would like to thank my advising professor, Dr K Lawrence. With his enthusiasm, his inspiration, and his great efforts to explain things clearly and simply, he helped to make research fun for me. I would have been lost without him.

I would also like to thank Dr. R. Kumar and Dr. S. Nomura for serving on my thesis committee. I thank Monal Patel and Urmi Khode for their valuable advice and friendly help. I also thank my roommates for creating a cordial environment and providing me with a strong support system. My deep gratitude to all my lab mates, who's continuous supported have encouraged me throughout my thesis.

I would like to thank my parents, Ashit Diwanji and Lina Diwanji who raised, supported, taught, loved and inspired me to earn things through hard work and sincerity. I would really like to thank my sister and brother-in-law whose support and love, has motivated me to accomplish my goals. I dedicate this thesis to my sister and brother-in-law.

November 22, 2010

ABSTRACT

AXIAL WAVE PROPAGATION IN TRUNCATED CONES

Bhumil A. Diwanji, M.S.

The University of Texas at Arlington, 2010

Supervising Professor: Kent L. Lawrence

While dealing with problems of impact analysis, where the force is dependent on the time, one can use the transient analysis to compute the response. Transient wave propagation has drawn interest from a long time mainly because of the way structural members behave when subjected to high rates of loading. Solutions to these problems find applications in the design of various mechanical equipments, or any situation where rigid objects are impacting on structural members.

The first part of this study deals with the axial wave propagation in cones of different apex angles using transient analysis in ANSYS. The results from the ANSYS are compared with existing analytical and experimental data available from other studies.

As the angle of the cone increases, the one dimensional modal theory fails to yield accurate results, due to lack of lateral inertia effects. The second part of this study is to examine at what angle the one dimensional theory for wave propagation ceases to be valid.

TABLE OF CONTENTS

LIST OF ILLUSTRATIONS

Figure Page

LIST OF TABLES

CHAPTER 1

INTRODUCTION

In the real world, all loads as well as the structural responses are time-varying. For example, a weight attached to a spring is released to vibrate freely; it will continue to vibrate until it reaches its steady state. If one is concerned only with steady state response, a static analysis is required, which neglects the dynamic effect of nature. The response before statics is called a transient state, in which dynamic effect cannot be neglected.

1.1 Literature Review

1.1.1 Experimental Investigations

In 1968, an experimental investigation was undertaken by V.H. Kenner and W. Goldsmith to study the propagation of waves produced by impact of projectiles on truncated 2024 aluminum cones with apex angles of 0.48, 5.38, 20, and 30 degree [5].The initial pulse incidence on the conical section was studied by gluing a cylindrical rod of the same diameter and material to the testing end of the cone. Only for the case of 20 degree cone, a piezoelectric crystal sandwiched between the apex end and the cylindrical frontal section of similar diameter was used for the same purpose. Wave propagation was initiated at the convergent end of all the cones as well as at the divergent end of the 0.48 and 5.38 degree cones by a striker. The axial impact on the cones was caused by a ½ inch diameter steel ball, fired at approximately 1300 ips with the help of a pneumatic gun or by just dropping it on the preceding cylindrical section of the cone. While in some cases the cone was struck directly to produce impact. The shape of the wave front and the velocity of the disturbance were also determined in the study. Surface strains were measured by means of foil and semiconductor resistance strain gages oriented along the direction of the generators of the cone. The velocity of the strikers was also derived

from the strain-gage records. The gages were bonded to the specimens using Eastman 910 or Epoxy 150 adhesive and no difference in the dynamic response of the gages mounted with either type of glue was found for the strain levels and frequencies of interest. The results indicated that one dimensional theory produced accurate results for smaller apex angles of 0.48 and 5.38 degrees where wave propagation in an elastic cone assumes no lateral inertial effects, shear and warping, where as it does not satisfies for large end cones of 20 and 30 degrees.

A similar study concerned with the impact on hollow cones was conducted by V.H. Kenner and W. Goldsmith along with J.L. Sackman, for investigating the effect of lateral inertia, on pulse durations of the elastic transient produced in a 20 degree apex angle hollow cone [10]. The general test arrangement and observation method were similar to the previous experiment with an exception that the cone was struck by the steel balls of different diameter. The conclusion of the study revealed that the accuracy of one dimensional theory progressively decreased with the decrease in pulse duration of the initial transient, as the theory overestimates peak amplitudes when the pulse length is shortened.

1.1.2 Numerical Analysis

In 1970, N. H. Sandlin [6] and C. Larson [7] published axial wave propagation in bars with variable cross sectional areas. N. H. Sandlin used one dimensional discrete parameter mathematical model together with a **simple predictor-corrector integration scheme** to investigate the propagation of waves along the longitudinal axis of rods. He considered the lumped mass model of a rod, which consisted of concentrated masses interconnected by springs of different spring constants, assuming springs had no mass density. He found solutions for free-free uniform rod, free-fixed uniform rod, stepped area rod, viscoelastic rod, elastic-plastic free fixed rod, 5.38 degree cone and 20 degree hollow cone. The forces applied in the models were a function of sine and sine square, with the number of nodes changing from 20 to 49 for different cases. He concluded his work by saying that, the most

disagreement between experimental and numerical data occurs in the free-free solid and hollow cone cases at points near the ends and at times following wave reflections; the discrepancy, may be due to a combination of inertia effects and inaccurate applied impulse force.

C. Larson in his thesis [7] applied a numerical method of modal superposition to develop a solution for wave propagation behavior in truncated cones. He used one dimensional elasticity theory to compute the results for solid cones with apex angles of 0.48, 5.38, 20 and 30 degrees and a hollow cone of 20 degree apex angle. The results acquired from his solutions were compared with one presented in Sandlin's thesis [6] and with experimental data obtained by Kenner and Goldsmith [5]. He concluded in his thesis that, the modal analysis solution is a reasonably good approximation for cones with apex angles less than thirty degrees and very good for angles less than about five degrees.

Both the authors compared their work with experimental investigation performed by Kenner and Goldsmith [5].

1.2 Project Motivation

The first major formulation of axial wave propagation in bars with variable cross sectional area was published in 1868 by M. B. De Saint-Venant [1]. Longitudinal impact analysis for rods has drawn interest for a long time mainly because of the need for information on the performance of structures subjected to high rates of loading. Solutions to these problems find applications in the design of various mechanical equipments, or in situation where rigid objects impact on structural members. For hundreds of years**,** longitudinal impact analysis has fascinated many famous scientists such as W. Goldsmith [2], K. F. Graff [3].

There has been a lot of research done by scientists and engineers on cylindrical rods or rods with uniform cross-sectional area along their length. However, for a rod with variable cross-sectional areas, there exist only few analytical solutions in the literature. According to B. Hu, P. Eberhard and W. Schielen [4],the main reason for this fact is due to the wave equation which

governs the solution to conical rods, is a partial differential equation with variable coefficients. The equation was very expensive to solve and required higher computational capable machines. Hence forth in past years, due to lack of computational capability many dynamics problems were modeled as lumped mass systems, making them easier and faster to solve. The lumped mass model of a rod, consisted of series of masses interconnected with springs of spring constants k. Spring constant, k is calculated using $k = \frac{AE}{L}$ where, E is Young's modulus, A is cross section area and L is the length of the rod. In the following study the accuracy of one-dimensional model with two-dimension model has been analyzed and it shows that the one-dimensional model does not yield accurate results for cone angles greater than about 10 degree.

Secondly, N Akkas, F Barez and W Goldsmith [11] performed investigation in elastic wave propagation in an exponential rod and 17.8° cone where in they found that for one-dimensional analysis the results diverges in the first and subsequent pulse reflections due to neglecting the effect of radial inertia. Similarly according to C. Larson [5], V.H. Kenner and W. Goldsmith [1] the two-dimensional elastic theory for determination of wave propagation in cones gives more accurate results than one-dimensional theory. Direct method for transient analysis has been used to check if the wave propagation yields the accurate results as modal superposition method that was used in previous studies.

1.3 Project Objectives

The study deals with the transient analysis of one-dimensional and two-dimensional models of the cone for different apex angles using ANSYS. There are two main motives behind investigating different apex angle cone models which are listed below

- Aim 1: At what angle does one- dimensional theory not apply for modal analysis?
- Aim 2: Analyze two-dimensional model of cone for wave propagation and compare its results with experimental and numerical results.

The results concluded in the study can be useful to any kind of impact analysis on the cone and can be utilized to determine the time needed for force to travel from one end of the cone to other.

The general overview of the thesis is stated below.

Chapter 2: Discusses setting up the model in ANSYS

Chapter 3: Discusses the results

Chapter 4: Discusses conclusion and future work.

CHAPTER 2

MODEL SETUP

2.1 Critical Frequency

To reduce computational time and produce simple inexpensive solution to complex formulation, it is always favorable to define a three-dimension model into one-dimension or two-dimension model. However, in modal analysis especially for the case of cones having large apex angle this is a drawback, as it ignores the lateral inertia effects, i.e. as the cone angle increases, error for frequency increases.

For solving the cases of transient analysis, the first few frequencies or modes affect the results significantly. According to Cook, Malkus, Plesha and Witt [8], the reduced mode set must include double the highest important frequency contained in the loading. For free-free analysis, the mode shapes are unrelated to complexity of loading. For all the solid cones, the pulse of force has duration of 35 microseconds. In this thesis, all the cones have free-free boundary conditions for which the critical frequency for mode of vibration is given by the set of equations given below.

$$Time\ constant\ T = 35\ X\ 10^{-6}\ Sec$$

$$Highest\ Freequency\ f = \frac{1}{T} = 28571.4\ Hz$$

$$Critical\ freequency = 2 * f = 57142.9\ Hz$$

2.1.1. One-Dimensional Model

Many dynamics problems in the past years are modeled as lumped mass systems because of its simple formulation and reduced computational time. Lumped mass model of the cone is considered as a series of masses m_i, connected by massless springs of spring constant

k_i. The parameters like m_i and k_i should be calculated carefully to reflect the approximate real time situation. Material of cone used for this study for analysis of one-dimension theory is aluminum with young's modulus of 10.6 x 10^6 psi and weight density of 0.1 lbf/in^3.

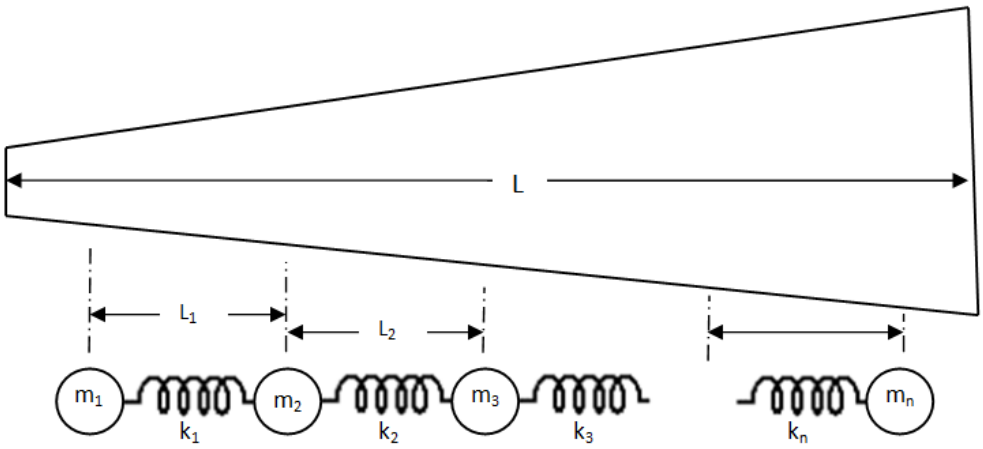

Mass(i) = Density * Volume(i)

$$\text{Volume(i)} = \frac{\pi * [r^2(i) + r(i) * r(i+1) + r^2(i+1)] * l}{3}$$

$$\text{Spring Constant k(i)} = \frac{A(i) * E}{L}$$

Figure 2.1 Lumped mass model

To determine, the accurate results of frequency for lumped mass model, proper amount of mesh elements are needed to be used. Use of higher number of meshing elements should be avoided because that will increase the computational time and space. The right mesh size can be determined by mesh refinements which converge to particular value. Appendix A shows the mesh convergence of lumped-mass model.

Matlab code [Appendix B] had been used to create the log file for ANSYS APDL. It can compute and create masses and spring constants for any number of nodes. This log file can run in ANSYS APDL to evaluate the different frequency results. One can compute as many

numbers of modes of frequency as required, but for this particular study the critical frequency has been considered below 58000 Hz.

2.1.2 Two-Dimensional Model

Modal analysis of ANSYS workbench has been used to solve the two dimensional axisymmetric model for all cone angles. Cone material has been considered as aluminum with young's modulus of 10.6×10^6 psi and weight density of 0.1 lbf/in^3. Mesh convergence has been checked. Appendix 2 provides the mesh convergence for different apex angles. Element size can be calculated by equation given below.

$$\text{Element size} = \frac{\text{Length of the cone}}{\text{Number of nodes}}$$

Table 2.1 Cone mesh density for 1D and 2D model

Degree cone	1D Model	2D Model	
	Number of nodes	Number of nodes	Number of elements
5.38	300	426	105
10	300	536	143
15	500	690	193
20	500	881	256

2.2 Comparison between Experimental and Two-Dimensional ANSYS model

To examine the reflection of a longitudinal wave pulse for free-free end conditions, two-dimensional axisymmetric model has been analyzed using ANSYS workbench software. For data comparisons truncated cones with apex angle of 0.48, 5.38, 20 and 30 degrees and hollow cone with apex angle of 20 degree has been considered.

According to R. Cook [8], in wave propagation and shock loading problems, many modes are excited and the response may be required for only a short period of time where direct method should be used. So, direct method for transient analysis has been used in

ANSYS workbench. Material of all the cones is aluminum with young's modulus of 10.6 x 10^{-6} psi and density of 0.1 lb/in^3. The meshes have been refined and converged in order to obtain accurate results. The element size of 0.24" has been considered for 0.48° and 5.38° solid cones, while element size of 0.06" has been used for remaining solid cones. For 20 degree hollow cone, mesh size of 0.06" has been used.

In wave propagation problem, to generate accurate results, time increment is an important factor. Time increment should be selected in such a way that, it includes an acoustic wave to transverse an element, for the element with the least transversal time. The time increment is calculated by equation 5 given by R. Cook [8]. For maximum ω critical frequency has been used.

$$\Delta t = \frac{2}{\omega_{max}}$$

$$\omega_{max} = 2 \times \pi \times 57142 = 359039 \ \frac{cycle}{sec}$$

$$\Delta t = 5.5 \times 10^{-6} \ sec$$

For solid cone with apex angle of 0.48 degree, the input pulse from experimental result was determined to be 33 microseconds half-sine pulse with peak load of 4500 pounds. The force is applied at the convergent end of the cone. The strain gauges were placed at 5.93 inch, 14.93 inch and 23.937 inches apart from the convergent end diameter.

Two cases have been considered for cone with apex angle of 5.38 degree. The force is applied both at the convergent end and divergent end of the cone. The input pulse from experimental result was determined to be 35 microseconds half-sine pulse with peak load of 5000 pounds applied at small end. And for divergent end, the input pulse was determined to be 35 microseconds half-sine square pulse with peak load of 5000 pounds. The strain gauges were placed at 1.5", 3.5" and 6" apart from small end diameter.

One solid cone and one hollow cone have been considered for apex angle of 20 degree. For solid cone, the input pulse from experimental result was determined to be 35

microseconds half-sine square pulse with peak load of 2500 pounds. For hollow cone, three different types of forces have been considered. One with peak load of 351 pounds, one with peak load of 127 pounds and one with peak load of 104 pounds with 50, 22 and 11 microseconds respectively half-sine square pulse. The force is applied at the divergent end of the cone. The strain gauges were placed at 1.477", 5.416" and 13.294" apart from divergent end diameter.

For cone with apex angle of 30 degree, the input pulse from experimental result was determined to be 40 microseconds half-sine pulse with peak load of 4500 pounds. The force is applied at the convergent end of the cone. The strain gauges were placed at 0.483", 6.283" and 9.083" apart from convergent end diameter.

CHAPTER 3

RESULTS

3.1 Comparison of Frequencies of One-Dimensional with Two-Dimensional Model

In Table 3.1 the frequencies of different cone angles for one-dimensional model are compared to two-dimensional model. Frequency below 58000 Hz has been considered for both models. For 5.38 degree cone angle, one-dimensional as well as two-dimensional model yields seven different modes of frequency. For 10 degree cone angle, one-dimensional model yields seven different modes of frequency while two-dimensional model yields nine different modes of frequency. For 15 and 20 degree cone angle, two-dimensional model yields ten and fourteen different modes of frequency respectively, while their one-dimensional model yields only seven different modes of frequency for both the cones. The difference in mode numbers occurs because one-dimensional model ignores radial inertial effects.

Table 3.1 Frequency comparison of different cone angles

Mode Number	5.38° cone		10 degree cone		15° cone		20 degree cone	
	1D	2D	1D	2D	1D	2D	1D	2D
1St	0	0	0	0	0	0	0	0
2nd	10918	10798	11388	11341	11598	11482	11708	11495
3rd	18943	18774	19619	19489	19952	19633	20134	19515
4th	26997	26790	27764	27466	28189	27414	28431	26507
5th	35134	34872	35919	35302	36404	34550	36696	27592
6th	43340	42985	44105	42907	44624	36278	44952	32665
7th	51597	51091	52322	50065	52858	40863	53212	37582
8th			---	53348	---	46141	---	41408
9th			---	56648	---	51012	---	44342
10th					---	54088	---	46076
11th							---	49075
12th							---	51194
13th							---	53671
14th							---	55863

Figure 3.1 shows, the percentage error in 1D model compare to 2D model frequency versus mode number for different cone angles. First mode has 0 Hz frequency because the geometry has free-free boundary condition. For 5.38 degree cone, the error in frequency is very less however after 15 degree, the error increases significantly. For 20 degree cone angle, the error is approximately 30% for seventh mode. The reason of this difference is also due to radial inertial effect. So after 15 degree cone angle, it is not advisable to use the one-dimensional theory.

$$\% \text{ Error} = \frac{\text{2D Frequency} - \text{1D Frequency}}{\text{2D Frequency}} \times 100$$

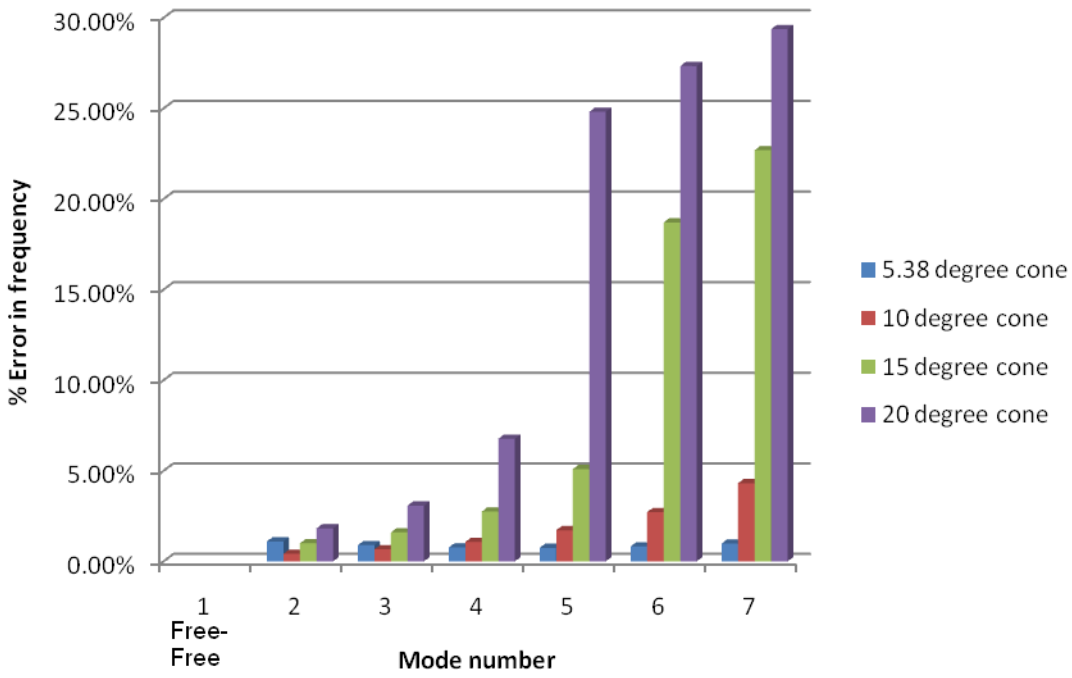

Figure 3.1 Percentage errors in 1D model compare to 2D model vs. mode number

3.2 Comparison of Experimental with ANSYS Results

The results from ANSYS workbench were compared with the experimental data, theoretical data and analytical solution for solid cones with apex angles of 0.48, 5.38, 20 and 30 degrees and hollow cone with apex angle of 20 degree.

3.2.1 For 0.48 Degree Solid Cone

The data shown in Figure 3.2 for 0.48 degree cone is compared to results documented by C. Larson [7] wherein he considered theoretical solution and experimental solution. The forcing function used for this cone is the same as one used by Larson. The maximum compressive strain at probe 1 is -1.98×10^{-3} in/in occurs at 46 microseconds, at probe 2 is 1.77×10^{-3} in/in occurs at 91 microsecond and at probe 3 it is 1.52×10^{-3} in/in occurs at 137

microsecond. While tensile strain occurs at $1.63x10^{-3}$ in/in at 192 microseconds for probe 3, at $1.79x10^{-3}$ in/in at 237 microseconds for probe 2.

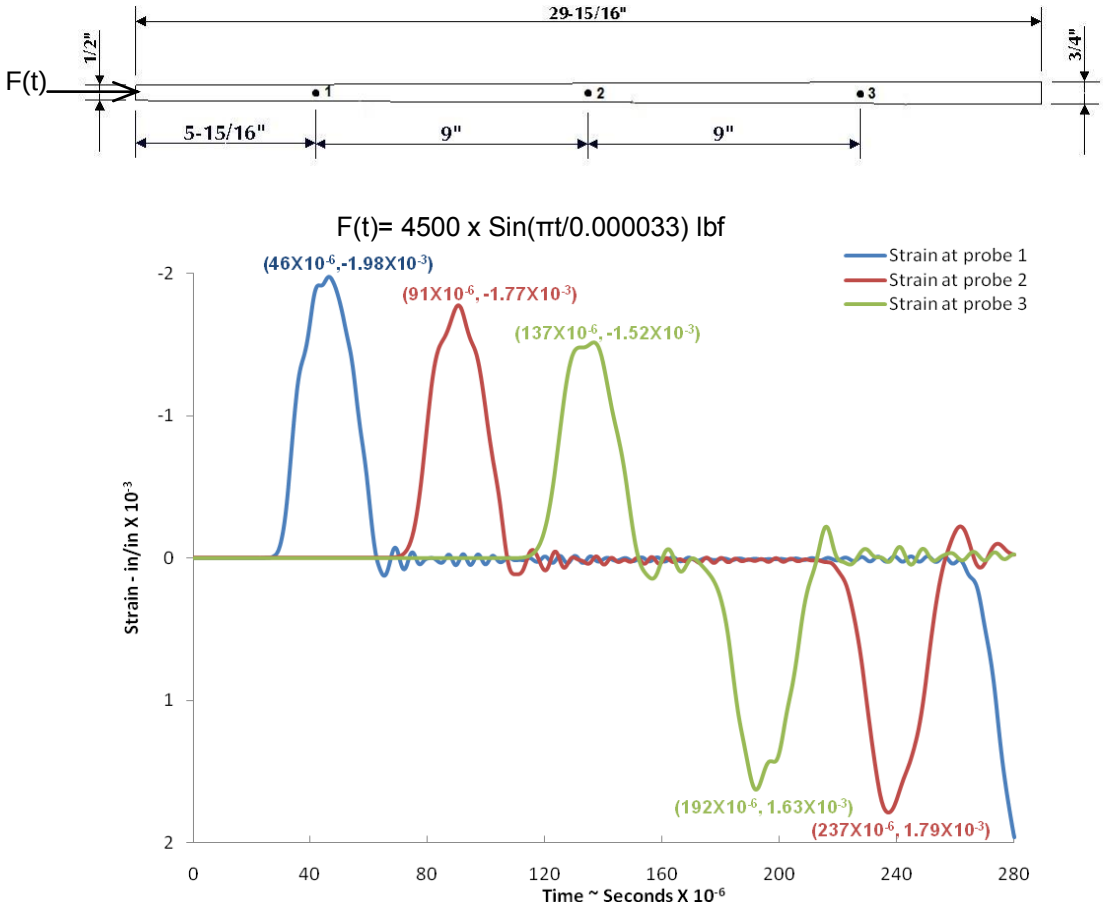

Figure 3.2 ANSYS calculated results for 0.48 degree solid cone

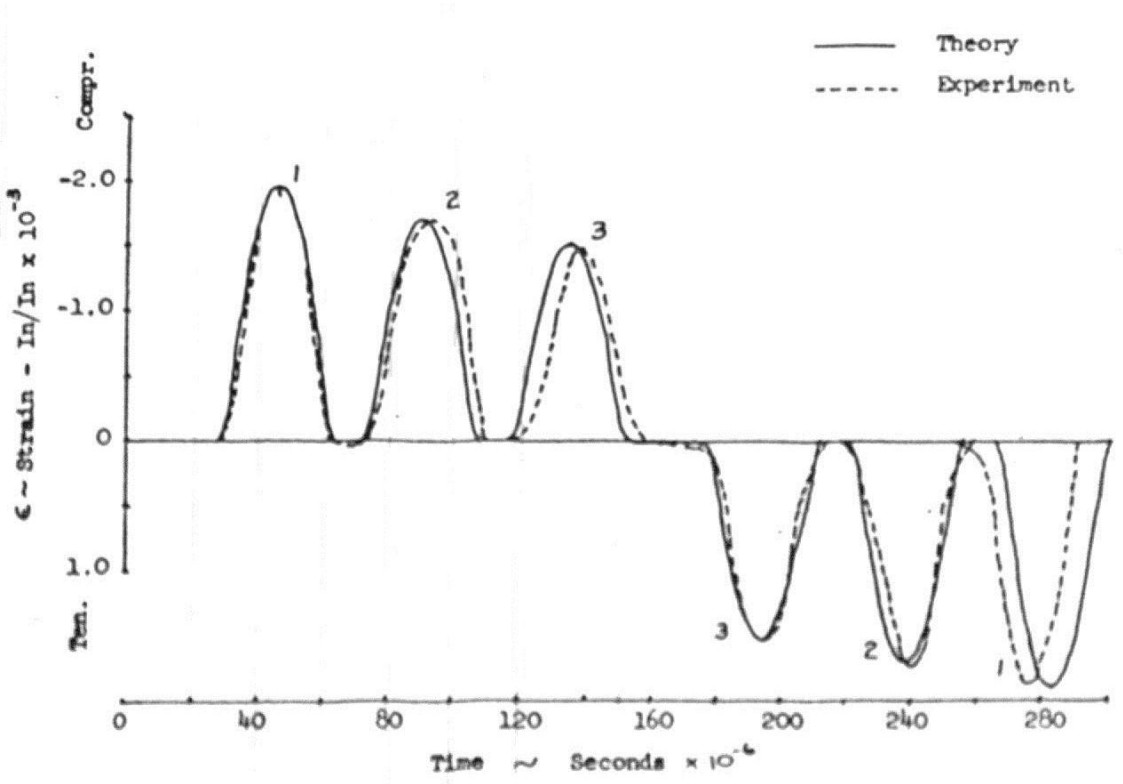

Figure 3.3 Theoretical and experimental results from Larson

3.2.2 For 5.38 Degree Solid Cone

Data shown in figure 3.4 for a 5.38 degree solid cone is compared to results documented by C. Larson [7] shown in figure 3.5. He had compared his solution with theoretical solution and numerical solution. The forcing function used for this cone is the same as one used by Larson and the force is applying at convergent end of the cone. From ANSYS result, the maximum compressive strain at probe 1 is 12.7×10^{-3} in/in occurs at 21 microseconds and 6.33×10^{-3} in/in occurs at 120 microseconds in tension, while theoretical and experimental results are approximately 12×10^{-3} in/in occurs at 21 microseconds for compressive and 5.75×10^{-3} in/in occurs at 120 microseconds. For probe 2, ANSYS results are 4.65×10^{-3} in/in occurs at 35 microsecond in compressive and 3.95×10^{-3} in/in occurs at 104 microseconds in tension while theoretical and experimental results are approximately 4.1×10^{-3} in/in occurs at 35 microsecond

in compressive and $3.5x10^{-3}$ in/in occurs at 105 microseconds in tension. For probe 3, ANSYS results are $2.19X10^{-3}$ in/in occurs at 63 microsecond in compressive and $2.3x10^{-3}$ in/in occurs at 85 microseconds in tension while theoretical and experimental results are approximately $2X10^{-3}$ in/in occurs at 66 microsecond in compressive and $1.5x10^{-3}$ in/in occurs at 86 microseconds in tension.

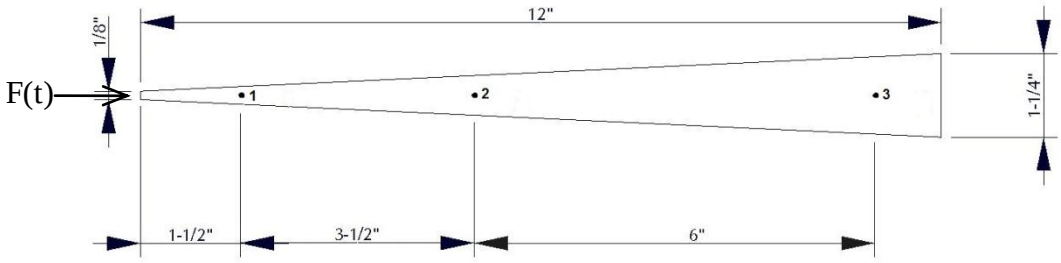

$F(t)= 5000 \times \sin(\pi t/0.000035)$ lbf

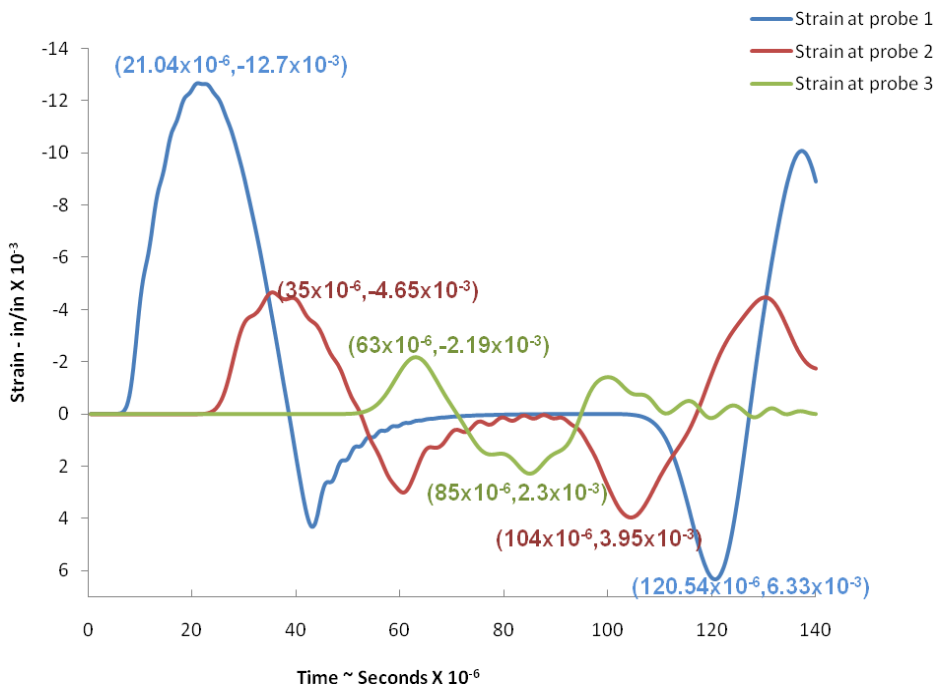

Figure 3.4 ANSYS calculated result for 5.38 degree solid cone

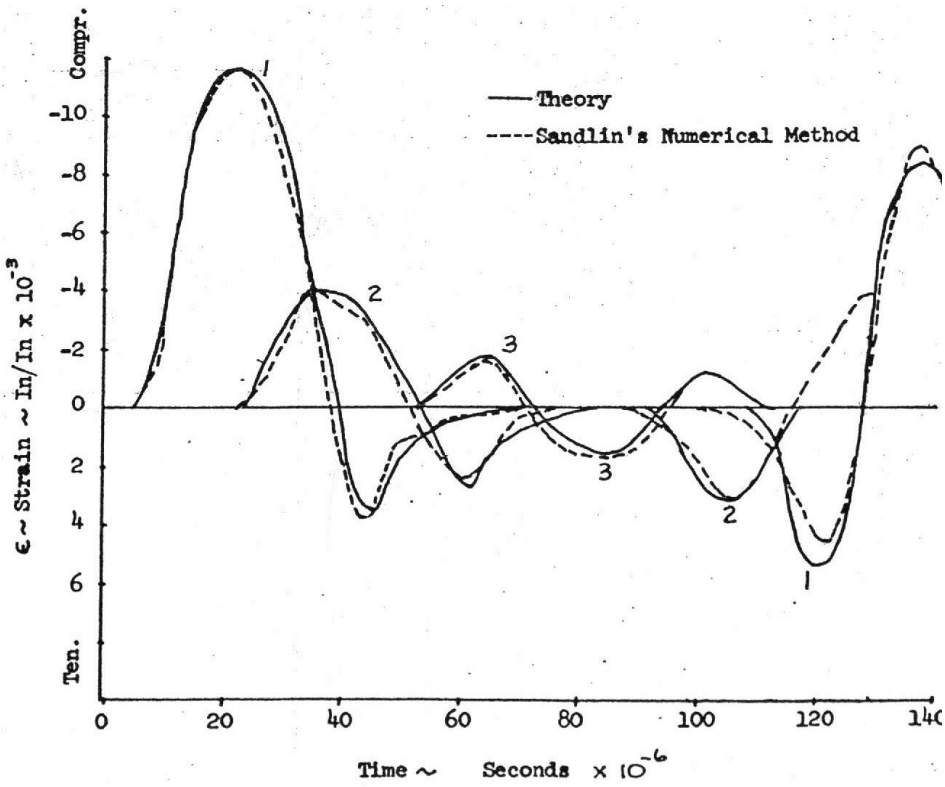

Figure 3.5 Theoretical and experimental results from Larson

Data shown in figure 3.6 for a 5.38 degree solid cone is compared to results documented by Sandlin [6] shown in figure 3.7. He had compared his solution with experimental results. The forcing function used for this cone is the same as one used by him and the force is applying at divergent end of the cone. From ANSYS result, the maximum compressive strain at probe 1 is 0.514×10^{-3} in/in occurs at 22.5 microseconds and 0.14×10^{-3} in/in occurs at 124 microseconds in tension, while numerical and experimental results are approximately 0.41×10^{-3} in/in occurs at 28 microseconds for compressive. For probe 2, ANSYS results are 0.69×10^{-3} in/in occurs at 42 microsecond in compressive and 0.44×10^{-3} in/in occurs at 104.5 microseconds in tension while numerical and experimental results are approximately 0.6×10^{-3} in/in occurs at 46 microsecond in compressive and 0.22×10^{-3} in/in occurs at 110 microseconds in tension. For probe 3, ANSYS results are 1.28×10^{-3} in/in occurs at 65.5 microsecond in compressive and 2×10^{-3} in/in occurs at 82 microseconds in tension while numerical and experimental results are

approximately $1x10^{-3}$ in/in occurs at 68 microsecond in compressive and $1.6x10^{-3}$ in/in occurs at 86 microseconds in tension.

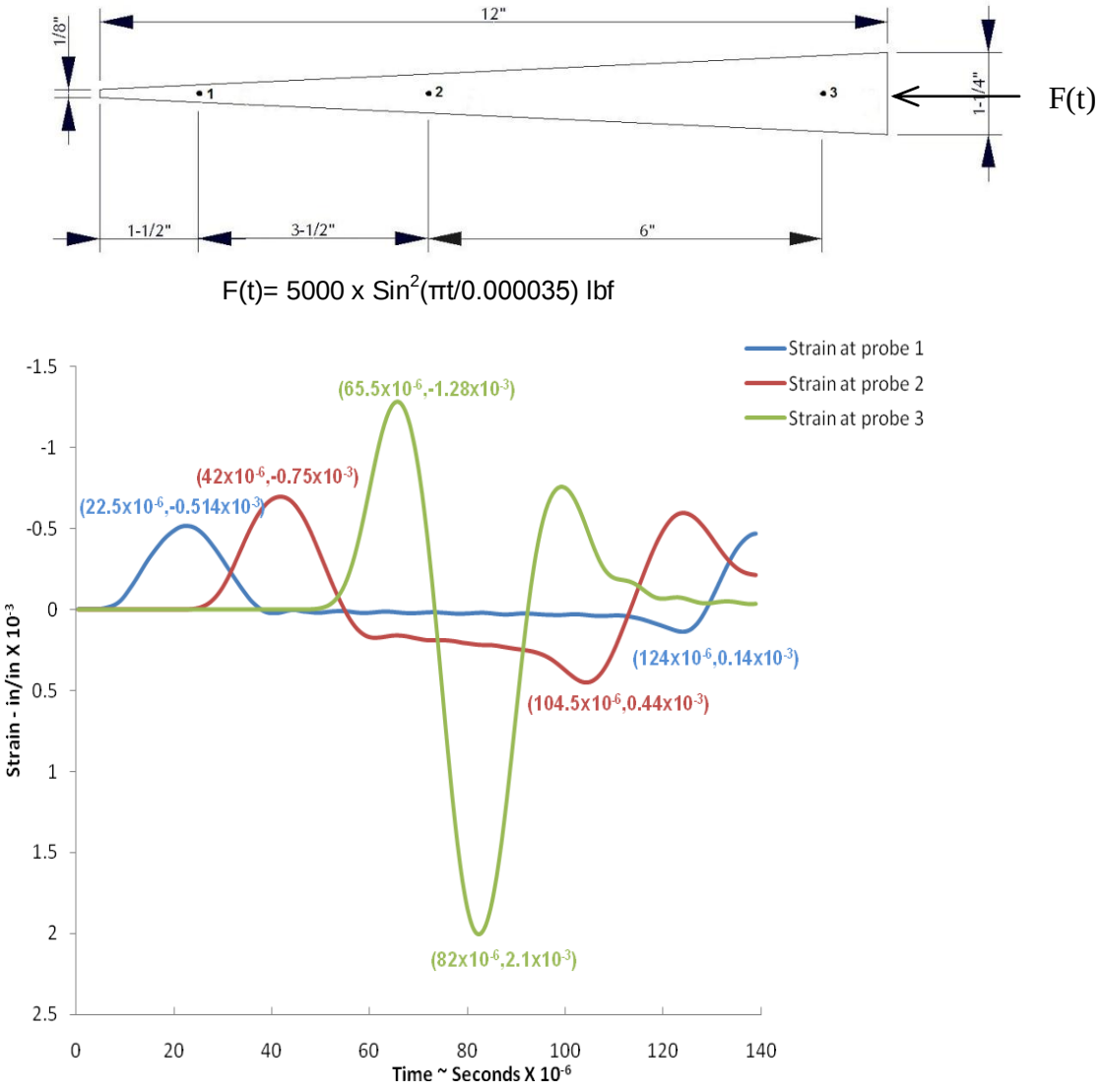

Figure 3.6 ANSYS calculated result for 5.38° solid cone stuck at divergent diameter

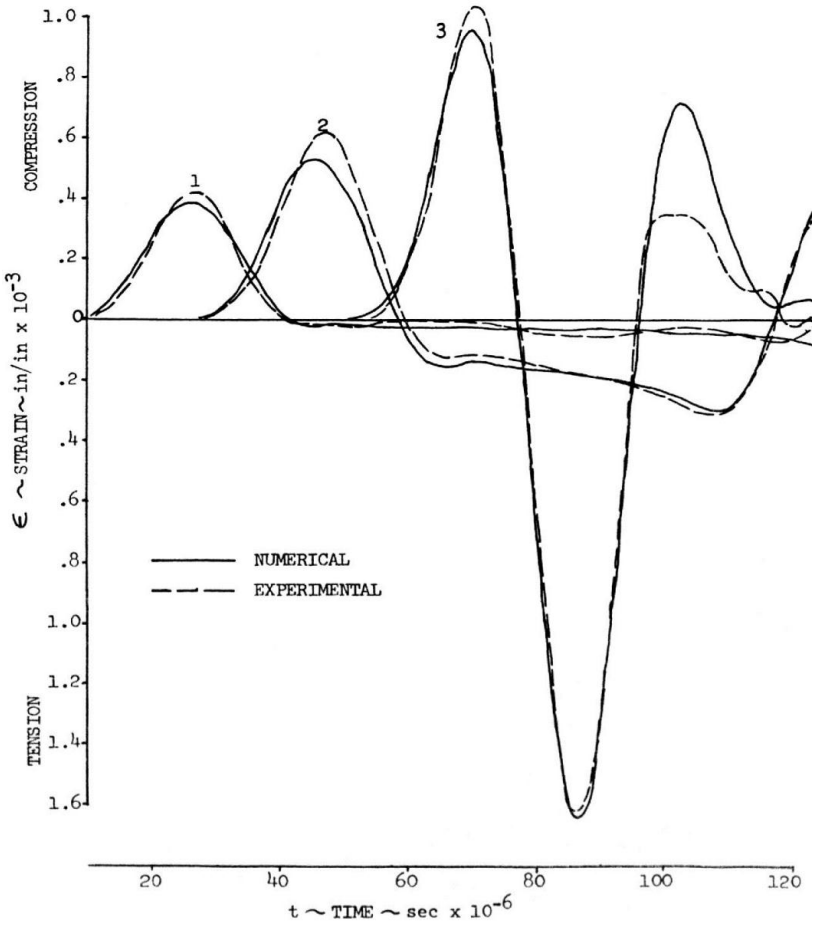

Figure 3.7 Numerical and experimental results from Sandlin

3.2.3 For 20 Degree Solid Cone

Data shown in figure 3.8 for a 20 degree solid cone is compared to results documented by Larson [7] shown in figure 3.9. He had compared his solution with experimental results. The forcing function used for this cone is the same as one used by him. From ANSYS result, the maximum compressive strain at probe 1 is 0.7×10^{-3} in/in occurs at 18 microseconds and 0.28×10^{-3} in/in occurs at 42 microseconds in tension, while theoretical and experimental results are approximately 0.65×10^{-3} in/in occurs at 20 microseconds for compressive and 0.25×10^{-3} in/in occurs at 40 microseconds for tension. For probe 2, ANSYS results are 0.22×10^{-3} in/in occurs at

38 microsecond in compression and $0.13x10^{-3}$ in/in occurs at 62 microseconds in tension while theoretical and experimental results are approximately $0.225x10^{-3}$ in/in occurs at 38 microsecond in compression and $0.15x10^{-3}$ in/in occurs at 60 microseconds in tension. For probe 3, ANSYS results are $0.068x10^{-3}$ in/in occurs at 83 microsecond in compression and $0.11x10^{-3}$ in/in occurs at 107 microseconds in tension while experimental results are approximately $0.1x10^{-3}$ in/in occurs at 80 microsecond in compression and $0.1x10^{-3}$ in/in occurs at 130 microseconds in tension.

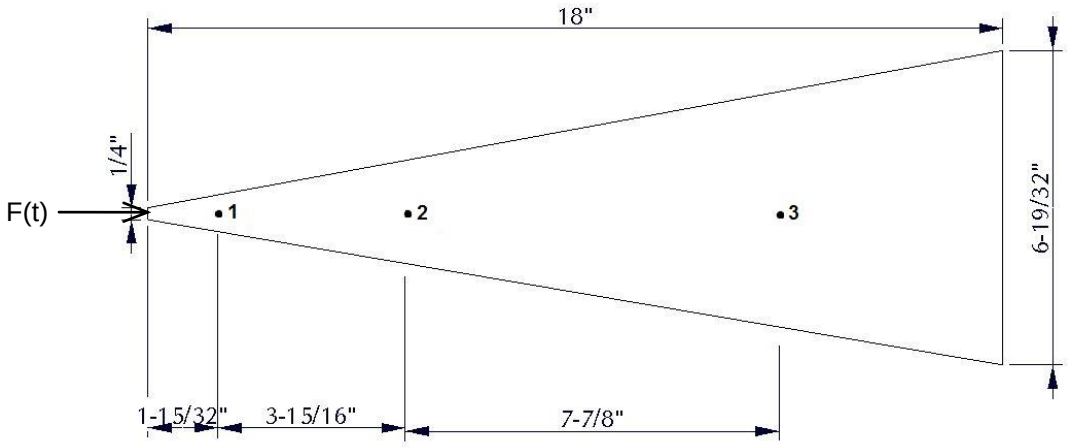

$F(t)= 2500 \times \sin^2(\pi t/0.000035)$ lbf

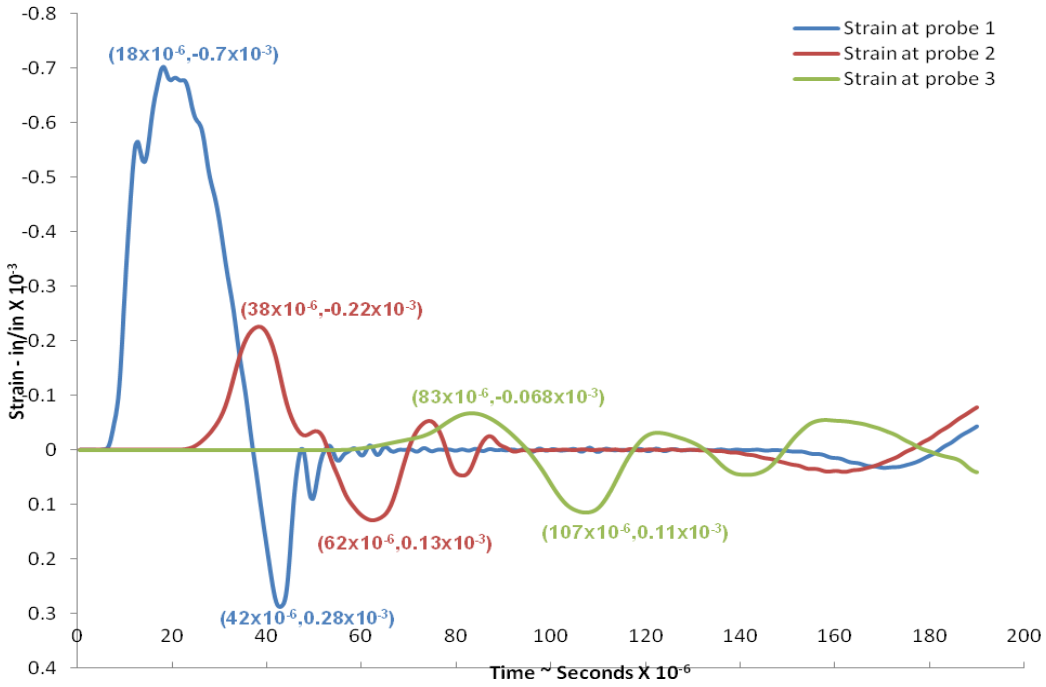

Figure 3.8 ANSYS calculated result for 20 degree solid cone

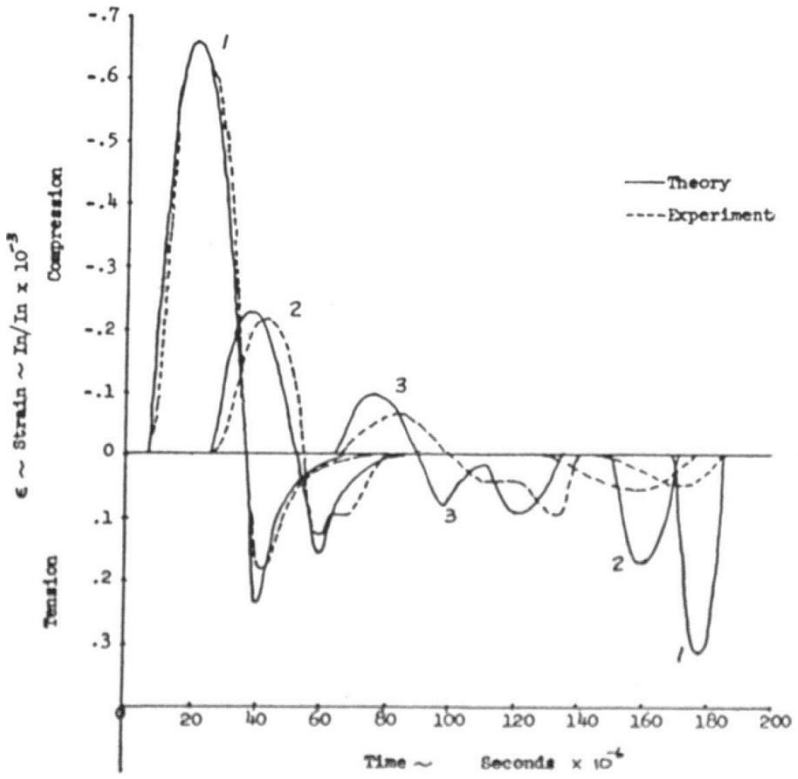

Figure 3.9 Theoretical and experimental results from Larson

3.2.4 For 30 Degree Solid Cone

Data shown in figure 3.10 for a 30 degree solid cone is compared to results documented by Larson [7] shown in figure 3.11. He had compared his solution with experimental results. The forcing function used for this cone is the same as one used by him. From ANSYS result, the maximum compressive strain at probe 1 is 1850×10^{-6} in/in occurs at 18.45 microseconds and 181×10^{-6} in/in occurs at 36 microseconds in tension, while theoretical and experimental results are approximately 1300×10^{-6} in/in occurs at 18 microseconds for compression and 181×10^{-6} in/in occurs at 42 microseconds for tension. For probe 2, ANSYS results are 164×10^{-6} in/in occurs at 48 microsecond in compression and 186×10^{-6} in/in occurs at 64 microseconds in tension while experimental results are approximately 100×10^{-6} in/in occurs at 30 microsecond in compression and 100×10^{-6} in/in occurs at 70 microseconds in tension. For

probe 3, ANSYS results are $176x10^{-6}$ in/in occurs at 100 microsecond in compression and $204x10^{-6}$ in/in occurs at 83 microseconds in tension while experimental results are approximately $100x10^{-6}$ in/in occurs at 100 microsecond in compression and $104x10^{-6}$ in/in occurs at 80 microseconds in tension.

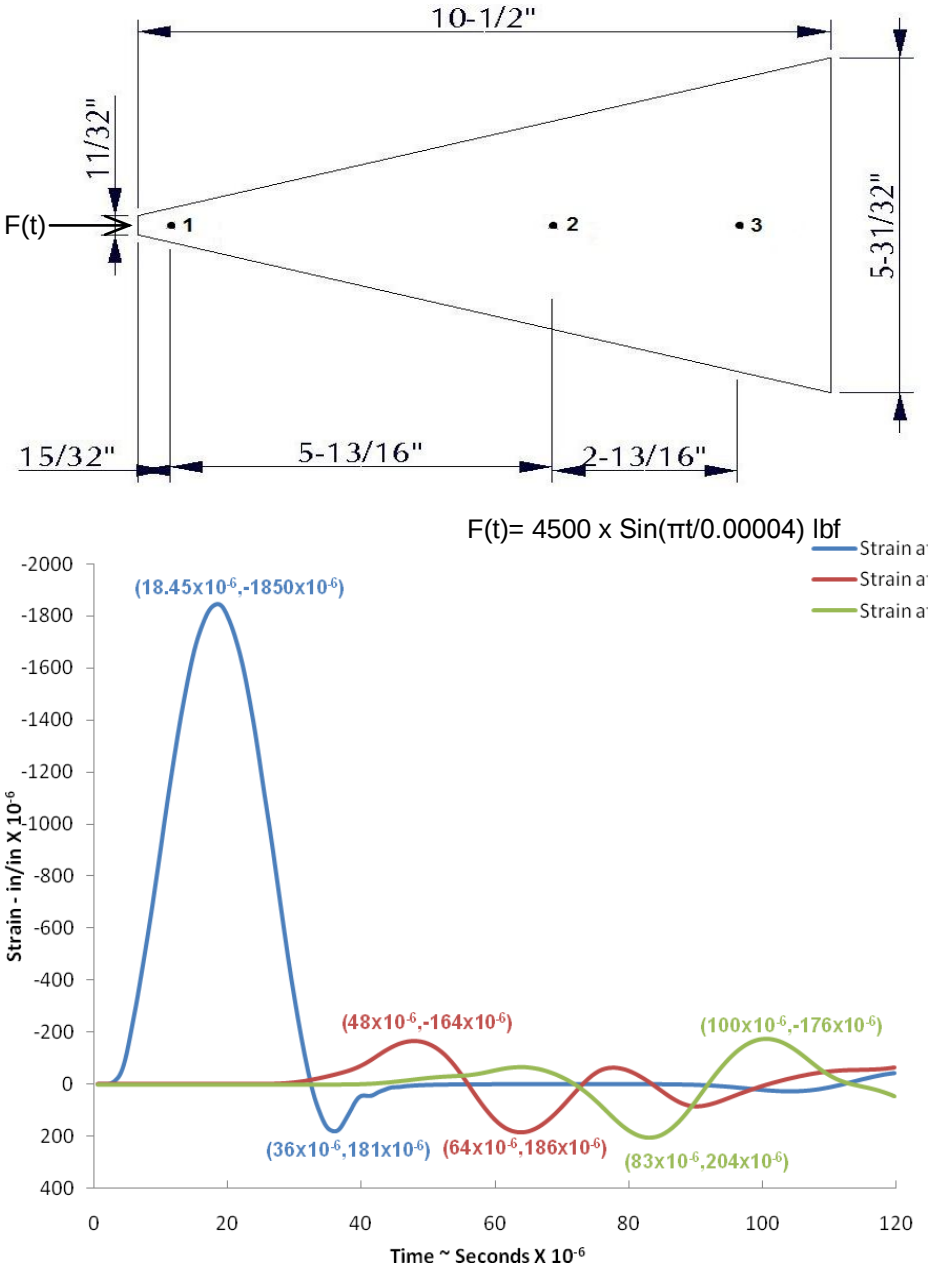

Figure 3.10 ANSYS calculated result for 30 degree solid cone

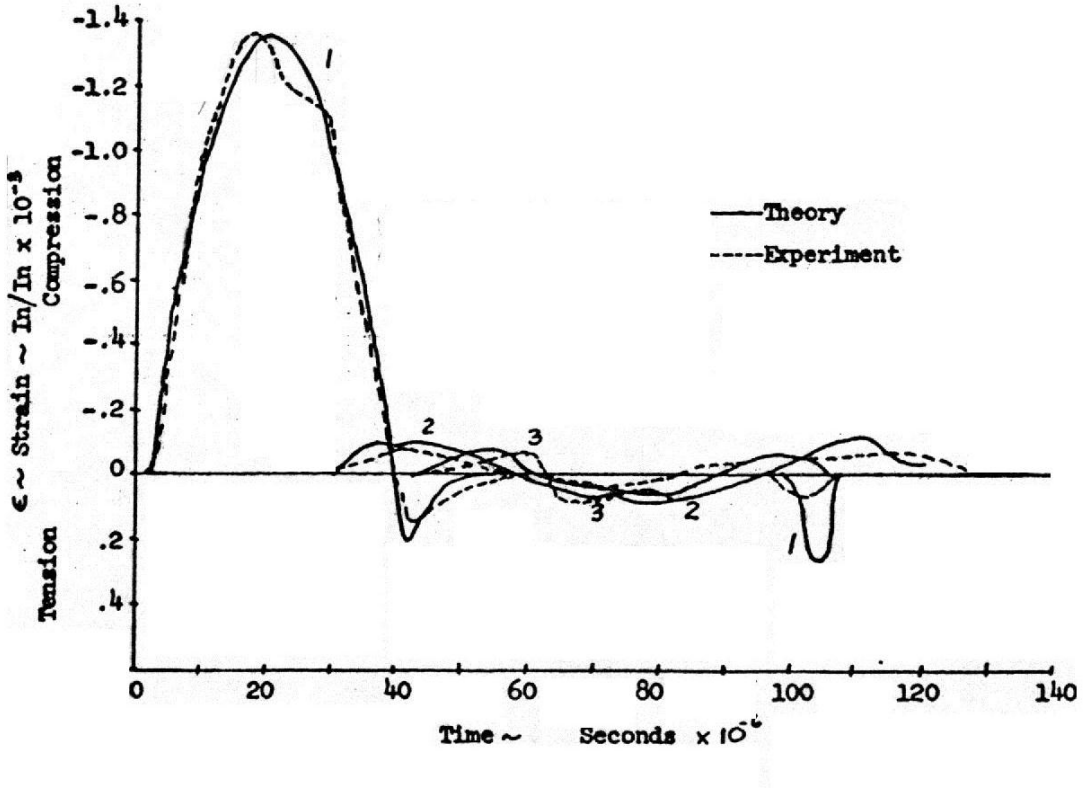

Figure 3.11 Theoretical and experimental results from Larson

3.2.5 For 20 Degree Hollow Cone

Three different forces has been applied to 20 degree hollow cone. Data shown in figure 3.12 for a 20 degree hollow cone is compared to results documented by Goldsmith [11] shown in figure 3.11. He had compared his solution with experimental results. The forcing function used for this cone is the same as one used by him. From ANSYS result, the maximum compressive strain at probe 1 is -67×10^{-6} in/in occurs at 30 microseconds while experimental results are approximately 65×10^{-6} in/in occurs at 28 microseconds for compression. For probe 2, ANSYS results are 35×10^{-6} in/in occurs at 51 microsecond in compression while experimental results are approximately 29×10^{-6} in/in occurs at 48 microsecond in compression. For probe 3, ANSYS results are 21×10^{-6} in/in occurs at 70 microsecond in compression while experimental results are approximately 20×10^{-6} in/in occurs at 68 microsecond in compression.

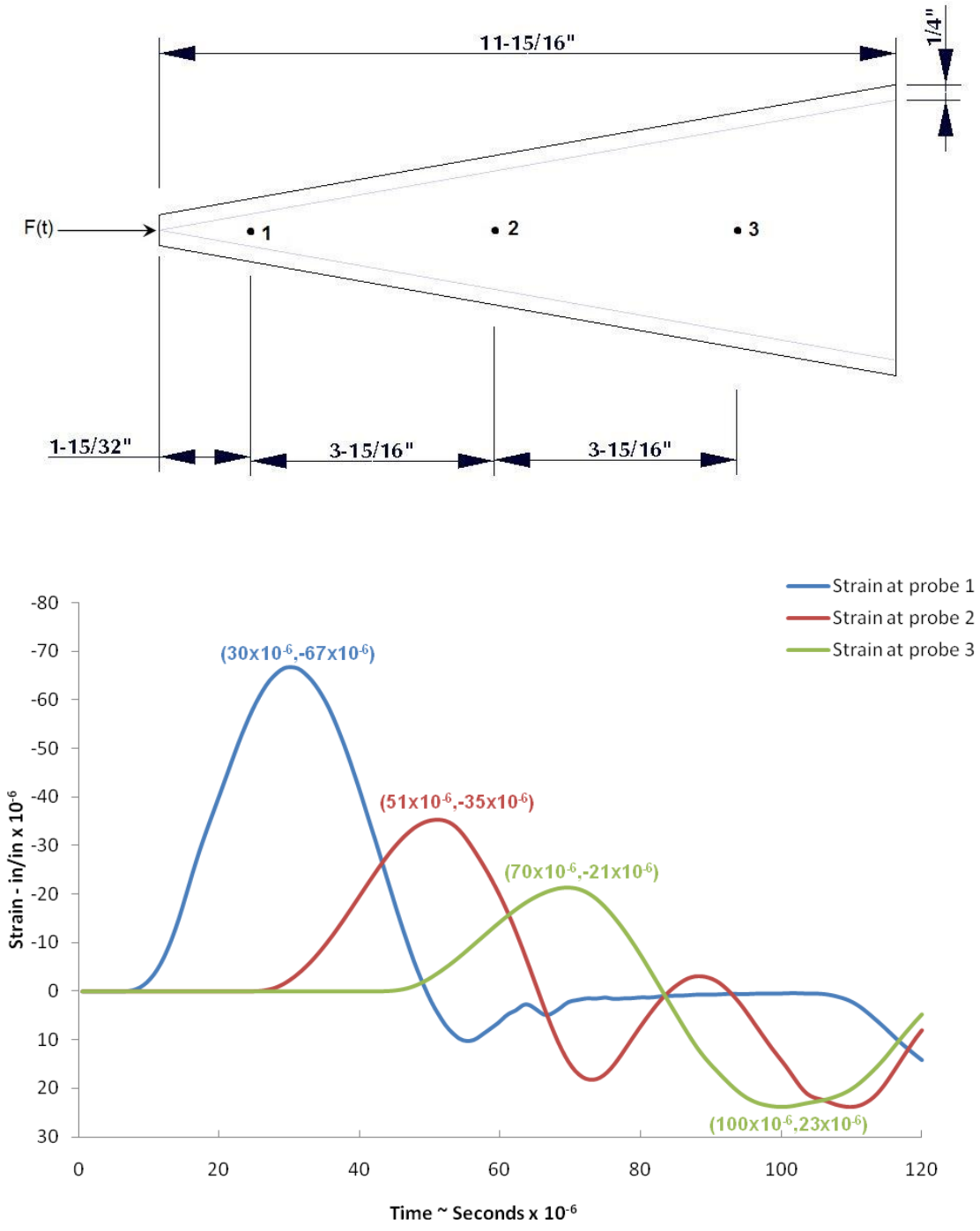

Figure 3.12 ANSYS calculated result for 20 degree hollow cone

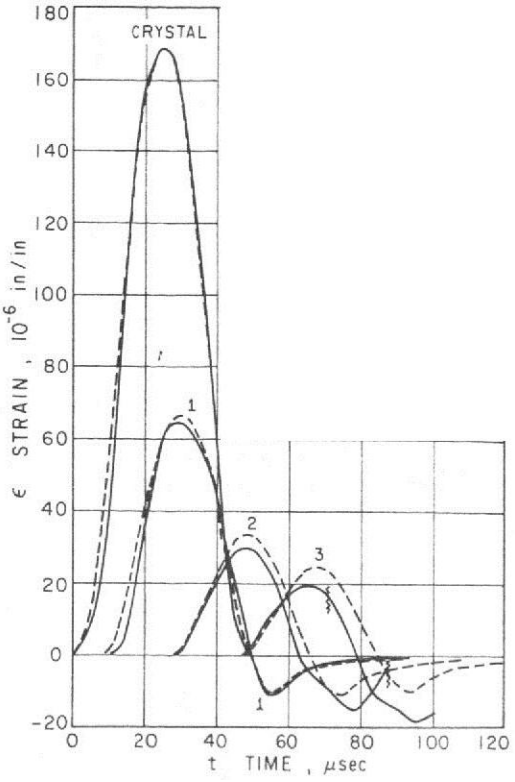

Figure 3.13 Experimental results by Goldsmith

Data shown in figure 3.14 for a 20 degree hollow cone is compared to results documented by Goldsmith [11] shown in figure 3.15. From ANSYS result, the maximum compressive strain at probe 1 is -30.6×10^{-6} in/in occurs at 17 microseconds while experimental results are approximately 25×10^{-6} in/in occurs at 18 microseconds for compression. For probe 2, ANSYS results are 11×10^{-6} in/in occurs at 37 microsecond in compression while experimental results are approximately 10×10^{-6} in/in occurs at 36 microsecond in compression. For probe 3, ANSYS results are 7×10^{-6} in/in occurs at 55 microsecond in compression while experimental results are approximately 6×10^{-6} in/in occurs at 55 microsecond in compression.

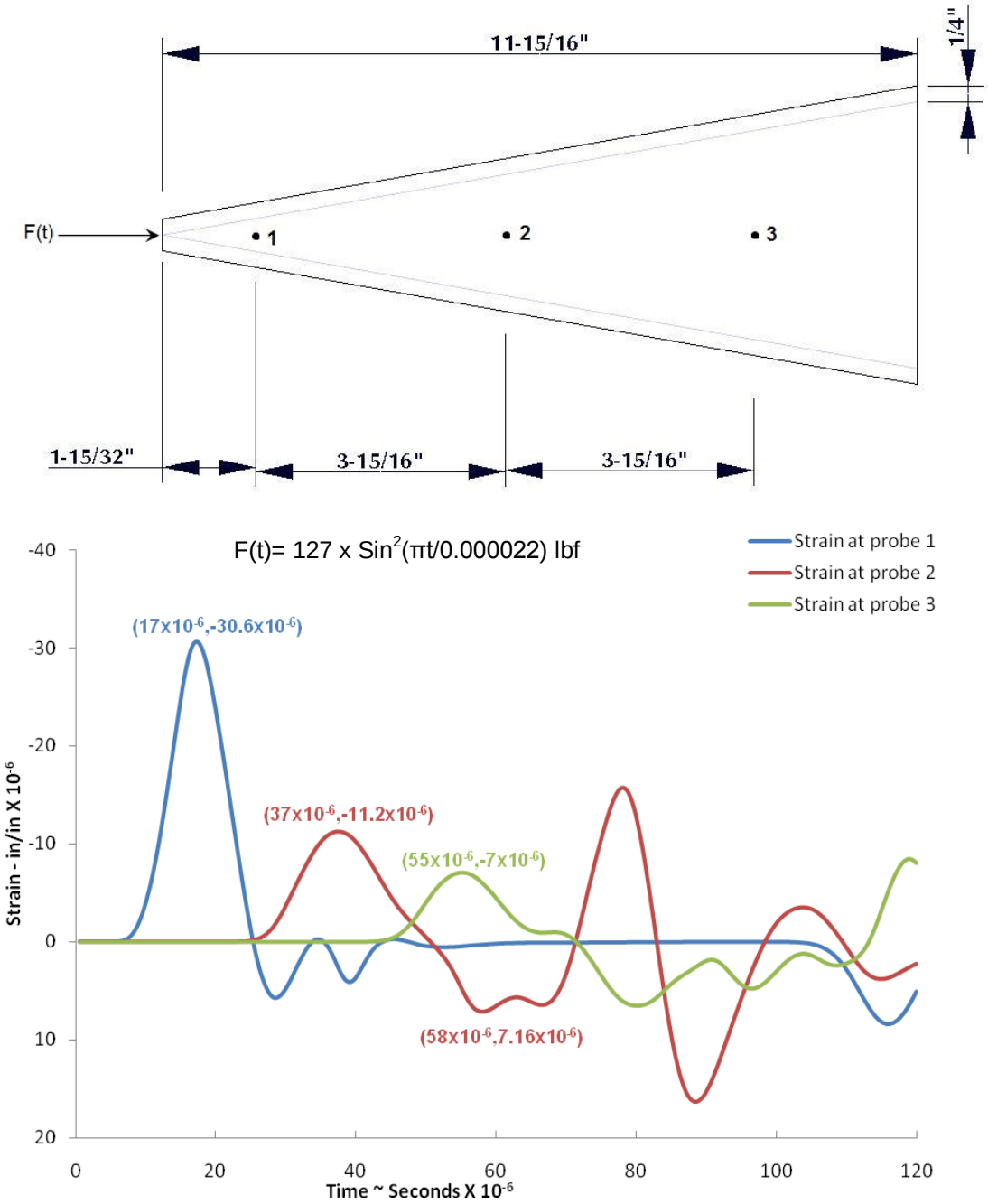

Figure 3.14 ANSYS calculated result for 20 degree hollow cone

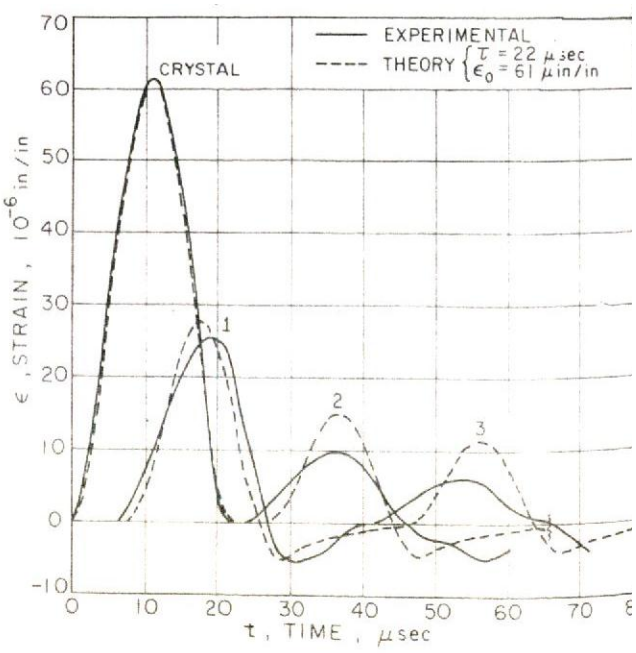

Figure 3.15 Experimental results by Goldsmith

Data shown in figure 3.16 for a 20 degree hollow cone is compared to results documented by Goldsmith [11] shown in figure 3.17. From ANSYS result, the maximum compressive strain at probe 1 is -25×10^{-6} in/in occurs at 14 microseconds while experimental results are approximately 25×10^{-6} in/in occurs at 13 microseconds for compression. For probe 2, ANSYS results are 8.5×10^{-6} in/in occurs at 31 microsecond in compression while experimental results are approximately 12×10^{-6} in/in occurs at 31 microsecond in compression. For probe 3, ANSYS results are 5.6×10^{-6} in/in occurs at 50 microsecond in compression while experimental results are approximately 10×10^{-6} in/in occurs at 51 microsecond in compression.

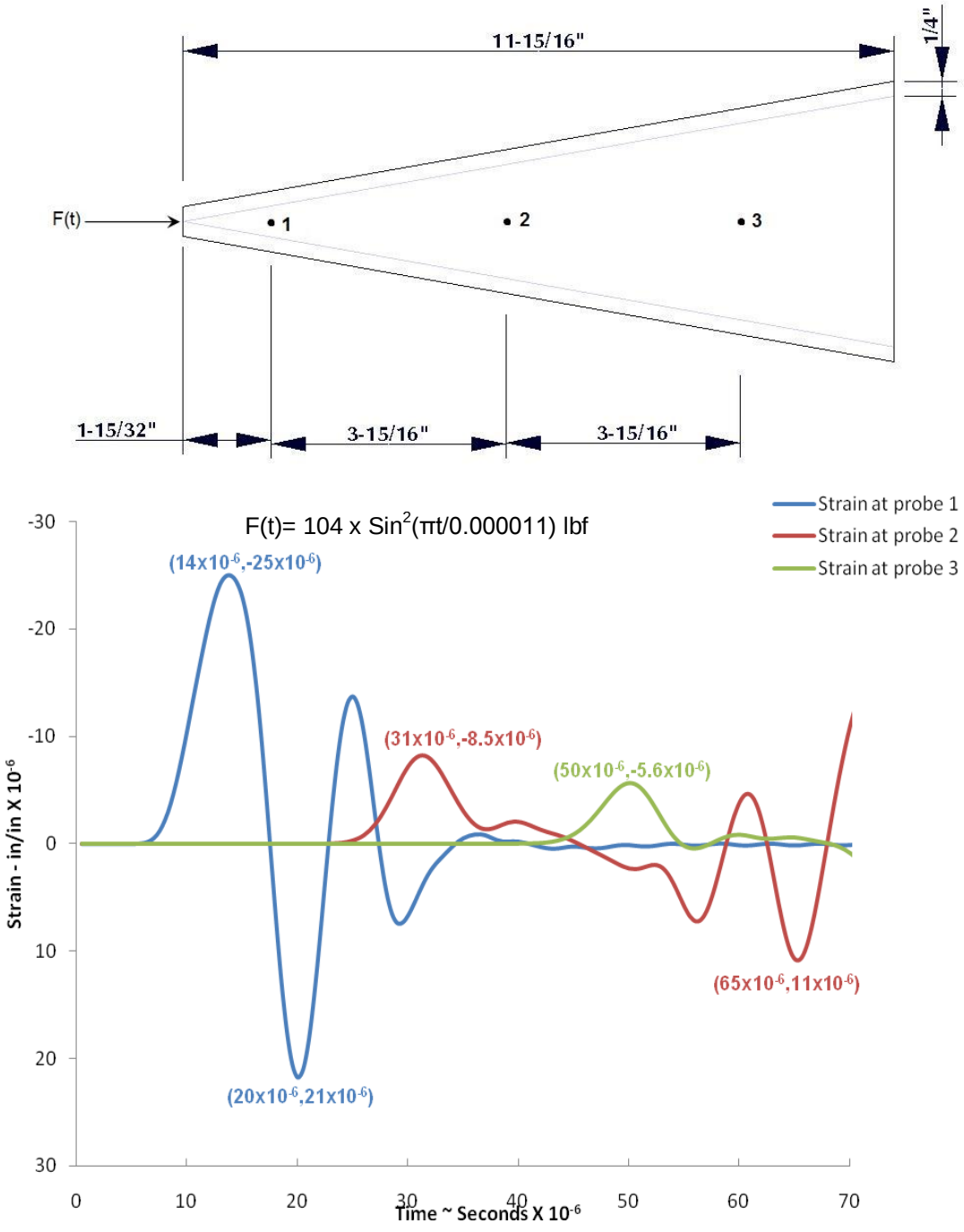

Figure 3.16 ANSYS calculated result for 20 degree hollow cone

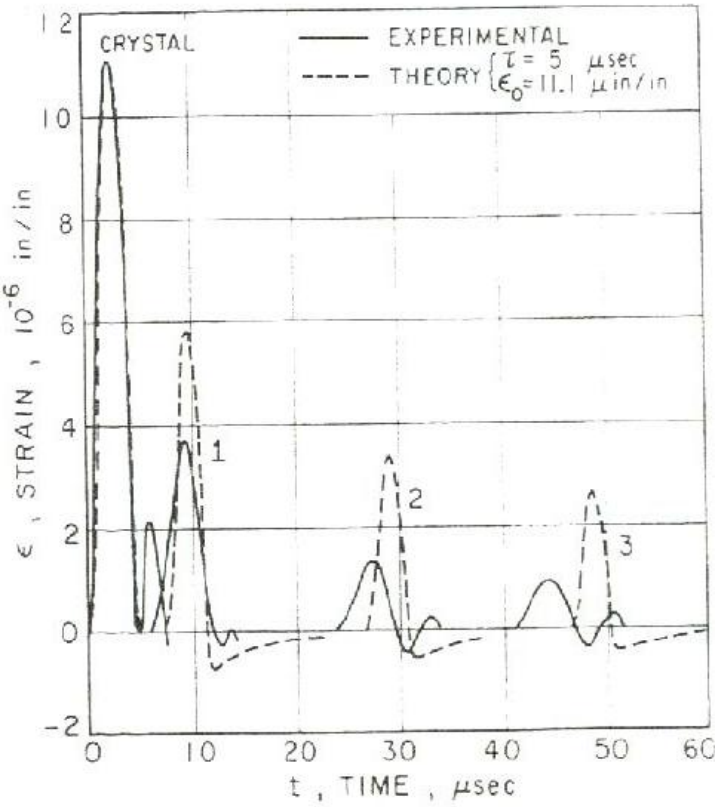

Figure 3.17 Experimental results by Goldsmith

CHAPTER 4

CONCLUSION AND FUTURE WORK

4.1 Limitations of One-Dimensional Theory

For the cone with apex angle of 10 degree and below, one-dimensional model yields accurate results. For the cone with apex angle of 20 degree, the results from one-dimensional model yields 30% error because one-dimensional model ignores radial inertia effect. Due to ignorance of radial inertia effect, one-dimensional model ignores a great number of mode shapes. For example, below 58000 Hz, for 20 degree cone, there were fourteen modes of frequency for two-dimensional model while for one-dimensional model there were only seven different modes of frequency. It is concluded that the one-dimensional theory is a reasonably good approximation for cones with apex angles less than 10 degree and really close agreement for angle less than 5°.

4.2 Discussion on Comparison of Experimental Results with ANSYS Results

The agreement of FEM results with experimental and numerical results is judged to be good. There are some minor difference in the results for all the cones, do not necessarily due to ANSYS setup, however it is assumed that difficulty in duplication exactly test conditions affect the comparisons.

The most serious disagreement between the ANSYS results and experimental results occurs in the free-free solid cases for 30 degree cone angle. The peak strain value for all the probes does not matches with experimental data but the time takes wave to travel yields the accurate results. That means, the peak value for applied force from experiment for 30 degree does a not match with applied ANSYS force.

4.3 Future Work

Although results indicate that, there is certain advantage of using two-dimensional axis symmetric model; the type presented here, however, three-dimensional model may give more accurate results. For future work, one can consider solution of three-dimensional model of the cone and compares with experimental data to check the deviation from two-dimension model.

APPENDIX A

MESH CONVERGENCE CHECK FOR ONE-DIMENSIONAL AND TWO-DIMENSIONAL MODEL

Table A.1 ANSYS APDL mesh convergence for 5.38 degree solid cone

ANSYS APDL Frequency									
Frequency	node	20	40	50	75	100	200	300	500
1st		2.3635E-04	7.7127E-04	0	1.1127E-03	0	2.66E-03	2.6100E-03	4.5123E-03
2nd		10875	10908	10912	10916	10917	10918	10918	10918
3rd		18772	18903	18918	18932	18937	18942	18943	18943
4th		26574	26897	26934	26970	26983	26995	26997	26998
5th		34288	34934	35008	35081	35106	35130	35134	35136
6th		41849	42986	43118	43246	43290	43333	43340	43344
7th		49186	51023	51236	51444	51516	51584	51597	51603

Table A.2 ANSYS workbench mesh convergence for 5.38 degree solid cone

ANSYS Workbench Frequency							
Frequency	Element size	0.6	0.3	0.24	0.16	0.12	0.06
1st		0	0	0	0	0	0
2nd		10798	10798	10798	10798	10798	10798
3rd		18774	18773	18773	18774	18774	18774
4th		26787	26790	26789	26789	26790	26790
5th		34873	34871	34871	34871	34872	34872
6th		42990	42984	42984	42984	42985	42985
7th		51083	51091	51092	51091	51091	51091

Table A.3 ANSYS APDL mesh convergence for 10 degree solid cone

ANSYS APDL Frequency						
Frequency	node	75	100	200	300	500
1st		1.11E-03	1.82E-03	1.96E-03	2.66E-03	7.66E-03
2nd		11385	11387	11388	11388	11388
3rd		19606	19612	19618	19619	19619
4th		27733	27748	27761	27764	27765
5th		35858	35887	35914	35919	35922
6th		43998	44048	44096	44105	44109
7th		52152	52232	52308	52322	52329

Figure A.4 ANSYS workbench mesh convergence for 10 degree solid cone

ANSYS Workbench Frequency							
Frequency	Element size	0.6	0.3	0.24	0.16	0.12	0.06
1st		0	0	0	0	0	0
2nd		11341	11341	11341	11341	11341	11341
3rd		19489	19489	19489	19489	19489	19489
4th		27467	27466	27466	27466	27466	27466
5th		35307	35302	35302	35302	35302	35302
6th		42915	42907	42907	42907	42907	42907
7th		50084	50065	50065	50065	50065	50065
8th		53322	53349	53348	53349	53349	53349
9th		56643	56648	56648	56648	56648	56648

Table A.5 ANSYS APDL mesh convergence for 15 degree solid cone

ANSYS APDL Frequency						
Frequency	Node	75	100	200	300	500
1st		1.00E-03	2.80E-04	3.01E-03	2.50E-03	5.14E-03
2nd		11594	11596	11597	11597	11598
3rd		19938	19945	19951	19952	19952
4th		28154	28170	28185	28187	28189
5th		36335	36367	36396	36402	36404
6th		44505	44559	44610	44620	44624
7th		52669	52754	52836	52851	52858

Table A.6 ANSYS workbench mesh convergence for 15 degree solid cone

ANSYS Workbench Frequency							
Frequency	Element size	0.6	0.3	0.24	0.16	0.12	0.06
1st		5.1995E-04	0.0000E+00	2.07E-03	1.6223E-03	2.64E-03	3.03E-03
2nd		11482	11482	11482	11482	11482	11482
3rd		19633	19633	19633	19633	19633	19633
4th		27415	27414	27414	27414	27414	27414
5th		34553	34550	34550	34550	34550	34550
6th		36271	36278	36278	36278	36279	36279
7th		40861	40863	40863	40863	40863	40863
8th		46143	46141	46141	46142	46142	46142
9th		51015	51012	51012	51012	51012	51012
10th		54101	54088	54088	54088	54088	54088

Table A.7 ANSYS APDL mesh convergence for 20 degree solid cone

ANSYS APDL Frequency						
Frequency	node	75	100	200	300	500
2nd		11704	11706	11707	11708	11708
3rd		20120	20127	20133	20134	20134
4th		28395	28412	28427	28430	28431
5th		36624	36656	36687	36693	36696
6th		44829	44884	44938	44947	44952
7th		53016	53104	53189	53204	53212

Table A.8 ANSYS workbench mesh convergence for 20 degree solid cone

ANSYS Workbench Frequency							
Frequency	Element size	0.6	0.3	0.24	0.16	0.12	0.06
2nd		11495	11495	11495	11495	11495	11495
3rd		19515	19515	19515	19515	19515	19515
4th		26508	26507	26507	26507	26507	26507
5th		27592	27592	27592	27592	27592	27592
6th		32663	32665	32665	32665	32665	32665
7th		37576	37581	37582	37582	37582	37582
8th		41404	41408	41408	41409	41409	41409
9th		44333	44341	44342	44342	44342	44342
10th		46092	46077	46076	46075	46075	46075
11th		49060	49074	49075	49075	49075	49076
12th		51199	51195	51194	51194	51194	51194
13th		53673	53671	53671	53671	53672	53672
14th		55886	55864	55863	55861	55861	55861

APPENDIX B

MATLAB CODE FOR ONE-DIMENSIONAL MODEL

```
clc
clear all
E=10.6e6;   %elastic modulus
d=0.1/386;       %density = 0.1
n=1000;       % no of nodes
ang=20;       %angle of cone in degree
L=12;       %length of cone
r1=0.0625;  %smallest cone radi
x=0.0625/tan(ang*pi()/(2*180));
new_L=L+x;
r2=tan(ang*pi()/(2*180))*new_L;         %largest cone radi
%r2=1.05;

l=12/(n-1);
inc=((r2-r1)*l/L);
fid = fopen('20degcone.txt', 'wb');        %to create new text file
name: 1D_run

fprintf(fid, '/batch\r\n');
fprintf(fid, '/prep7\r\n\r\n');
fprintf(fid, 'n, 1, 0, 0\r\n');
g(1)=0;                                    %to write location of nodes in
text file

for i=2:n

    g(i)=g(i-1)+l;
    fprintf(fid, 'n, %d, %f, 0\r\n', i, g(i));
end
fprintf(fid,'\r\n');
fprintf(fid, 'et, 1, combin14\r\n');
fprintf(fid,'et, 2, mass21, 0,0,4\r\n\r\n');

for i=1:n-1                                %calculating spring constant
and write in the text file
    r(1)=r1;
    r(i+1)=r(i)+inc;
    A(i)=3.14*(r(i)*r(i)+r(i+1)*r(i+1))/2;
    K(i)=A(i)*E/l;
    fprintf(fid,'r, %d, %e, , ,\r\n',i,K(i));
    fprintf(fid, 'type, 1\r\n');
    fprintf(fid, 'real, %d\r\n', i);
    fprintf(fid, 'en, %d, %d, %d\r\n\r\n',i,i,i+1);
end

for i=1:n-1
    Vol(i)=pi()*(r(i)*r(i)+r(i)*r(i+1)+r(i+1)*r(i+1))*l/3;
    m(i)=d*Vol(i);

end
```

```
mass=zeros(n,1);
mass(1)=m(1)/2;
mass(n)=m(n-1)/2;
for i=2:n-1
    mass(i)=m(i)/2+m(i-1)/2;
end

for i=1:n
    fprintf(fid,'r, %d, %e,\r\n',n-1+i, mass(i));
    fprintf(fid, 'type, 2\r\n');
    fprintf(fid, 'real, %d\r\n',n-1+i);
    fprintf(fid, 'en, %d, %d\r\n\r\n',n-1+i, i);
end

for i=1:n
    fprintf(fid, 'd, %d, uy,0\r\n', i);
end

% fid=fopen('try2.txt','wb');
%
% for i=1:n-1
%     fprintf(fid,'%f %f\r\n',mass(i));
% end

fclose(fid);
h(1)=mass(1);                              %to find the mass
for i=2:n
    h(i)=h(i-1)+mass(i);
end
```

REFERENCES

1. Isaac Todhunter and Karl Pearson, “A History of the Theory of Elasticity and of the Strength of Materials,” Vol. II, Part II, p. 289, Dover Publications, New York, 1960, p. 92.

2. Werner Goldsmith, “Impact: The Theory and Physical Behaviour of colliding solids,” London Edward Arnold Ltd, 1960.

3. Karl F. Graff, “Wave Motion in Elastic Solids,” Ohio State University Press, 1975.

4. B. Hu, P. Eberhard and W. Schiehlen, “Symbolical Impact Analysis for a Falling Conical Rod against the Rigid Ground”, Journal of Sound and Vibration, 240(1), pp. 41-57, 2001.

5. V. H. Kenner and W. Goldsmith, “Elastic waves in truncated cones”, Experimental Mechanics, Vol. 8, No. 10, Springer Boston Publication, pp. 442-449, 2006.

6. Ned H. Sandlin, “Numerical Calculation of Longitudinal Pulse Propagation in Rods”, MS thesis, The University of Texas at Arlington, 1970.

7. Charles E. Larson, “Axial Wave Propagation in Bars With Variable Cross Sectional Area Using Modal Analysis”, MS thesis, The University of Texas at Arlington, 1970.

8. Robert D. Cook, David S. Malkus, Michael E. Plesha, Robert J. Witt, ”Concepts and Applications of Finite Element Analysis”, John Wiley & Sons, 2002.

9. J.S. Wu, M. Hsieh and C. L. Lin, “A Lumped-Mass Model for the Dynamic Analysis of the Spatial Beam-Like Lattice Girders”, Journal of Sound and Vibration, Vol 228, Issue 2, pp. 275-303, 1999.

10. V. H. Kenner, J. L. Sackman and W. Goldsmith, “Longitudinal Impact on a Hollow Cone”, ASME Paper No. 69, pp. 445-450, 1969

11. Nuri Akkas and Freidoon Barez and Werner Goldsmith, “Elastic Wave Propagation in an Exponential Rod”, Journal of Mechanical Science, Vol. 22, Pergamon Press Ltd., pp. 199-208, 1979.

BIOGRAPHICAL INFORMATION

Bhumil Diwanji was born in Gujarat, India in July 1985. He attended The University of Texas at Arlington, Texas where he received his B.S. in Mechanical Engineering and graduated as Cum Laude. He is currently working on his M.S. in Mechanical Engineering at UT Arlington. He also served as a Graduate Teaching Assistant for two years for subjects like Computer Aided Design and Machine Design.